



OPEN Construction and evaluation of a diagnostic model for Alzheimer's disease based on mitophagy-related genes

Jiarui Liu^{1,3}✉, Mengyu Yan^{2,3}, Lihua Chen¹, Weihua Yu²✉ & Yang Lü¹✉

Alzheimer's disease (AD) is the most common cause of dementia. Mitophagy fulfills crucial functions in neurodegenerative disorders and neuronal survival but the relationship between mitophagy and AD is unclear. Mitophagy correlation scores between AD samples and control samples were calculated using single-sample GSEA (ssGSEA) based on two datasets from gene expression omnibus (GEO) database. Mitophagy-related genes (MRGs) and differentially expressed genes (DEGs) in AD screened by WGCNA and "limma" package were intersected to take common genes. These overlapping genes were further compressed and used for diagnostic modeling by adopting the recursive feature elimination (RFE) and LASSO analysis. The reliability of the diagnostic model was verified based on the receiver operating characteristic (ROC) curve. Then, a transcription factor (TF)-mRNA regulatory network of these key genes was established. Lastly, ssGSEA was employed to examine the relationship between the identified genes and cellular pathways and immune cell infiltration. AD samples had notably lower mitophagy correlation scores than control samples. A total of 12 MRGs in the module with the greatest mitophagy connection with AD patients were identified. Functional enrichment analysis revealed that the DEGs were significantly enriched in synaptic function-related pathways. Based on GSE122063, a diagnostic prediction model was created and validated using two mitophagy-related genes (*YWHAZ* and *NDE1*), showing an area under ROC curve (AUC) greater than 0.7. This confirmed that the diagnostic model had a high predictive value. The TF-mRNA network showed that four TFs, namely, *FOXC1*, *FOXO1*, *HOXA5* and *GATA2*, were regulated by both *YWHAZ* and *NDE1* genes. Immune infiltration analysis revealed that *NDE1* promoted the infiltration of most immune cells, while *YWHAZ* mainly inhibited the infiltration of most immune cells. The current findings improved our understanding of mitophagy in AD, contributing to future research and treatment development in AD.

Keywords Alzheimer's disease, Mitophagy, WGCNA, Biomarkers, Diagnostic model

Abbreviations

AD	Alzheimer's disease
MRGs	Mitophagy-related genes
RFE	Recursive feature elimination
A β	Amyloid β peptide
p-tau	Hyperphosphorylated tau
WGCNA	Weighted gene co-expression network analysis
GS	Gene significance
MM	Module affiliation
DEGs	Differentially expressed genes
CC	Cellular component
MF	Molecular function
BP	Biological process
GO	Gene ontology

¹Department of Geriatrics, The First Affiliated Hospital of Chongqing Medical University, Chongqing 400016, China. ²Institute of Neuroscience, Chongqing Medical University, Chongqing 400016, China. ³Jiarui Liu and Mengyu Yan have contributed equally to this work. ✉email: liujiarui66666@163.com; yuweihua@cqmu.edu.cn; yanglyu@hospital.cqmu.edu.cn

KEGG	Kyoto encyclopedia of genes and genomes
KM	Kaplan–Meier
AUC	Area under ROC curve
DCA	Decision curve analysis
GEO	Gene expression omnibus
LASSO	Least absolute shrinkage and selection operator
ROC	Receiver operating characteristic
GSVA	Gene set variant analysis
ssGSEA	Single-sample gene set enrichment analysis
YWHAZ	Neurodevelopmental protein 1
NDE1	Neurodevelopmental protein 1
FOXL1	Forkhead box L1
FOXC1	Forkhead box C1
HOXA5	Homology box A5
GATA2	GATA-binding protein 2
EC	Endothelial cell
TEMRA	T effector memory CD45RA+
BBB	Blood–brain barrier

Alzheimer's disease (AD) is a neurological condition associated with advanced progressive dementia and is characterized by cognitive impairments and progressive, irreversible memory loss¹. As the most common form of dementia, AD accounts for 60–80% of all dementia cases in this century². Currently, AD affects 50 million patients worldwide, ranking the sixth leading cause of mortality². The World Health Organization reported that the prevalence of AD increases with age, peaking at 25–50% among the elderly and roughly 5–8% among those aged over 65. By 2050, AD will impact about 115 million individuals globally if current trends continue³. Patients with advanced AD experience severe malnourishment, multiple organ failure due to neuronal necrosis, and even brain death⁴. Diagnostic methods of AD currently include cerebrospinal fluid protein analysis and positron emission tomography of tracer molecules⁵. However, since pathological changes begins decades before the manifestation of clinical symptoms⁶, it is critical to find reliable biomarkers for an early detection of AD in order to improve patients' pathological changes and cognitive deficits⁷.

Mitochondria are an organelle that functions as the power plant to cells. It has been discovered that the development of neuroplasticity is significantly influenced by mitochondria. Specifically, mitochondria control axonal development and differentiation during early neural differentiation by buffering cytoplasmic Ca^{2+} to promote axonal microtubule polymerization⁸. Hyperphosphorylated tau (p-tau) and amyloid β peptide (A β) have been shown to accumulate during AD pathogenesis as a result of mitochondrial malfunction and neuronal bioenergetic abnormalities. Neuronal apoptosis and mitochondrial abnormalities can be facilitated by A β and p-tau pathology^{9,10}. Thus, the health of neurons depends on maintaining mitochondrial homeostasis, which can be achieved by various mechanisms of mitochondrial quality control, such as mitophagy. This process involves the phagocytosis and breakdown of damaged mitochondria^{11,12}. Mitophagy has been shown to be essential for neuronal survival and function through preserving a healthy mitochondrial pool and preventing neuronal death^{13,14}. Memory loss and AD pathogenesis can be exacerbated by the buildup of defective mitochondria caused by impaired mitophagy. By preventing A β and p-tau buildup, mitophagy restoration improves memory loss in an AD mouse model^{15,16}. Thus, mining mitophagy-related gene (MRG) biomarkers for AD diagnosis could help overcome the treatment bottleneck of the disease.

Based on the transcriptomic data of AD patients collected from the GEO public database, this study conducted an in-depth analysis to develop a MRG-related signature using machine learning algorithms, including weighted gene co-expression network analysis (WGCNA). Additionally, the robustness of the model was confirmed using external data. Furthermore, a TF-mRNA interaction network was established and the expressions of feature genes in AD were determined. Finally, the relationship between immune cell infiltration and biological pathways and the identified genes was analyzed. In conclusion, our study may provide new perspectives and strategies for the detection of AD and its treatment.

Methods

Data acquisition

The scRNA-seq expression profiles of AD in GSE132903¹⁷ and GSE122063¹⁸ scRNA-seq expression profiles were sourced from GEO (<https://www.ncbi.nlm.nih.gov/geo/>) database. Specifically, GSE132903 samples were from the middle temporal gyrus and some of the GSE122063 samples were from the frontal lobe. Based on the platform annotation files of microarray data, the probe-level expression profiles were translated into gene-level expression profiles. When numerous probes matched to the same gene, the average of those probes was computed as the gene expression, whereas the probe was eliminated if one probe matched to many genes. The maximum value obtained from several probes matching to one gene was considered as the gene's expression value. Samples without status or clinical follow-up information were excluded while retaining samples with a survival time of more than 30 days. After preprocessing, the data of GSE132903 (training set: AD = 97; Controls = 98) and GSE122063 (test set: AD = 56; Controls = 44) were acquired. Finally, 34 MRGs from a previous literature were extracted for further analysis¹⁹.

WGCNA construction

WGCNA, a systems biology technique, could characterize the patterns of gene correlation among various samples to identify highly synergistically varying gene sets and candidate biomarker genes or therapeutic targets. This

study developed a weighted gene co-expression network based on 195 diseased and control samples utilizing the “WGCNA” software²⁰ to find co-expression networks and select genes from various clusters.

The autophagy-related score of the dataset GSE132903 was evaluated using the ssGSEA method, and the autophagy-related gene set was used as the background gene set to calculate the autophagy score of the training set samples. The R software package “WGCNA” software²⁰ was used to identify the autophagy-related gene modules of patients with AD, and the ssGSEA scoring results were used as traits to perform WGCNA analysis on the training set. Using the WGCNA’s “pickSoftThreshold” R function, the ideal soft threshold power was determined to ensure the network’s scalability. Subsequently, the adjacency matrix was transformed into a topology matrix, which was further converted into an adjacency matrix. Average-linkage hierarchical clustering approach was adopted based on the topological overlap measure to cluster the genes²¹. After identifying the gene modules using the dynamic shear method, we determined the eigenvector values (eigengenes) of each module and combined close modules into a new one by setting height = 0.25, deepSplit = 2, and minModuleSize = 80. Then, based on gene significance (GS) and module affiliation (MM), the “WGCNA” software was employed to analyze the interaction strengths to reflect the relationship between the gene modules and AD patients²². To assess module-trait interactions based on the correlations between the module genes and clinical trait, the “Heatmap” software²³ was applied to extract various module-characterized genes according to the first principal component (PC) of module expression. Next, genes with the strongest positive or negative module-trait connections were selected. Furthermore, the genes obtained from the modules were imported into the STRING database (Version: 12.0) for protein–protein interaction (PPI) analysis²⁴ under CONFIDENCE ≥ 0.4 .

DEGs analysis

Robust multi-array average (RMA) approach in the “affy” R package²⁵ and Bioconductor package were adopted to perform background correction, quantile normalization, and professional summarization of gene expression profiling data derived from the 195 samples. Using the “limma” program^{26–28}, gene expression data were determined to identify those whose expression significantly changed between AD and control samples. Under the thresholds set to $|\log_2\text{FC}| \geq 1$ and $\text{padj} < 0.01$, significant DEGs were filtered using the “limma” package²⁹. DEGs were visualized using the “ggplot2” program³⁰ into a volcano plot. Finally, the overlapping genes of the DEGs and the module genes obtained by WGCNA were extracted.

Screening MRGs-related feature genes to develop a diagnostic model and validation

Further perform LASSO regression and Recursive Feature Elimination (RFE) on overlapping genes. Specifically, LASSO regression in R language’s “glmnet” package³¹ was performed to reduce the gene number while retaining genes. Take the characteristic genes at the intersection of LASSO and RAF as the biomarkers of this study and establish a diagnostic model. Then, the R package “timeROC”³² was employed to compute the AUC and show time-dependent receiver operating characteristic (ROC) curves to evaluate the efficacy of the biomarkers in differentiating AD from control samples in the training set GSE132903 and the test set GSE122063.

Establishment of a TF-mRNA regulatory network

By accessing JASPAR (<https://jaspar.elixir.no/>), a TF motif database, the TFs of biomarkers were predicted using the NetworkAnalyst (<https://www.networkanalyst.ca/>) to create a TF-mRNA interaction network. Cytoscape (version 3.7.2)³³ was employed to visualize their interactions.

Immune infiltration analysis

We used ssGSEA³⁴ to calculate the enrichment scores of 28 types of immune cells in each sample³⁵. Using Spearman’s correlation coefficient, the relationship between immune cell infiltration and the biomarkers was compared.

Functional enrichment analysis

In functional enrichment analysis, Gene Ontology (GO) uses cellular component (CC), molecular function (MF), and biological process (BP) terms to characterize the roles of genes and proteins. Kyoto encyclopedia of genes and genomes (KEGG) stores the information about systemic, chemical and genetic functions^{36–39}. Here, the primary activities and signaling pathways of the DEGs were analyzed by performing functional enrichment analyses. Using the R program “clusterProfiler”⁴⁰, the GO and KEGG functions of DEGs were analyzed. The Top 10 functions enriched in BP, MF, and CC terms in the GO enrichment and the top 20 enriched KEGG pathways were visualized. The bubble plot of the top 20 pathways in the KEGG pathway enrichment results was plotting employing the “GSVA” software package⁴¹. And based on the results of functional enrichment analyses, ssGSEA scores were computed to evaluate the correlation between biomarkers and the pathway scores. The pathways of h.all.v2023.2.Hs.symbols.gmt were collected from GSEA website (<http://www.gsea-msigdb.org/gsea/index.jsp>).

Statistical analysis

Statistical analyses were performed using R software (version 3.6.0). Differences in continuous variables between two groups were analyzed by the Student’s t-test (parametric test) or the Wilcoxon rank-sum test (non-parametric test). The correlation between biomarker expressions and immune scores was measured by Spearman correlation analysis. $*p < 0.05$, $**p < 0.01$, $***p < 0.001$, and $****p < 0.0001$ denoted a statistical significance, while ns indicated $p > 0.05$. The flowchart of this study can be seen in Fig. S1.

Results

Screening MRGs-related genes by WGCNA

Using the list of MRGs as the background gene set, it was found that all of the AD samples in the dataset had considerably lower mitophagy-related scores than the control samples (Fig. 1A). Next, we identified gene modules linked to mitophagy in AD patients using WGCNA, with ssGSEA score as the traits against the training set. According to the module correlations, no modules could be merged, and the soft threshold β was determined to be 12 by the pickSoftThreshold function ($R^2 = 0.9$, Fig. 1B). Nine modules were identified when the minimum number of genes in a module was 80, and no notable outlier samples were discovered (Fig. 1C). A heat map of the module-shape correlation was visualized (Fig. 1D). The association between modules and mitophagy data was analyzed to identify clinically significant modules. The nine modules included 2932 genes, with the MEbrown module showing the strongest association with mitophagy ($\text{cor} = 0.67$ and $p = 1.17 \times 10^{-26}$), therefore this significant module was chosen for further study. Using brown color to represent the MEbrown module, a strong positive correlation between MM and GS ($\text{cor} = 0.66$, $p < 1. \times 10^{-200}$, Fig. 1E) was detected. Next, 39 genes with $|\text{GS}| > 0.75$ and $|\text{MM}| > 0.75$ that were closely related to mitophagy were identified. These genes were imported into the STRING database for analyzing PPIs after removing genes without interactions ($\text{CONFIDENCE} \geq 0.4$). The gene interaction relationships and confidence scores are shown in Table S1. Finally, 12 genes were included as the modular MRGs for subsequent investigation.

Identification of DEGs and functional analysis

417 DEGs (257 down-regulated and 160 up-regulated genes) was obtained (Fig. 2A). Next, a gene expression heatmap for the top 100 DEGs from both AD and control samples was generated to investigate the relationships between the DEGs and the clinical features (gender, female/male, age, $\leq 80 / > 80$ years). A negative correlation in the expression patterns of up- and down-regulated genes was observed (Fig. 2B). GO and KEGG functional enrichment analysis showed that the DEGs were significantly enriched to neurotransmitter transport, neurotransmitter secretion, synaptic vesicle recycling, signal release, and synaptic signal release in BP term (Fig. 2C). In CC term, the genes were mostly enriched to presynapses, glutamatergic synapses, synapses across neurons, transport vesicle membranes, and transport vesicles (Fig. 2C). In MF term, the DEGs were most significantly enriched to binding, GTPase activity, SNARE binding, calmodulin binding, and protein C-terminal binding (Fig. 2C). Moreover, the DEG were significantly enriched to the pathways of gap junction pathways,

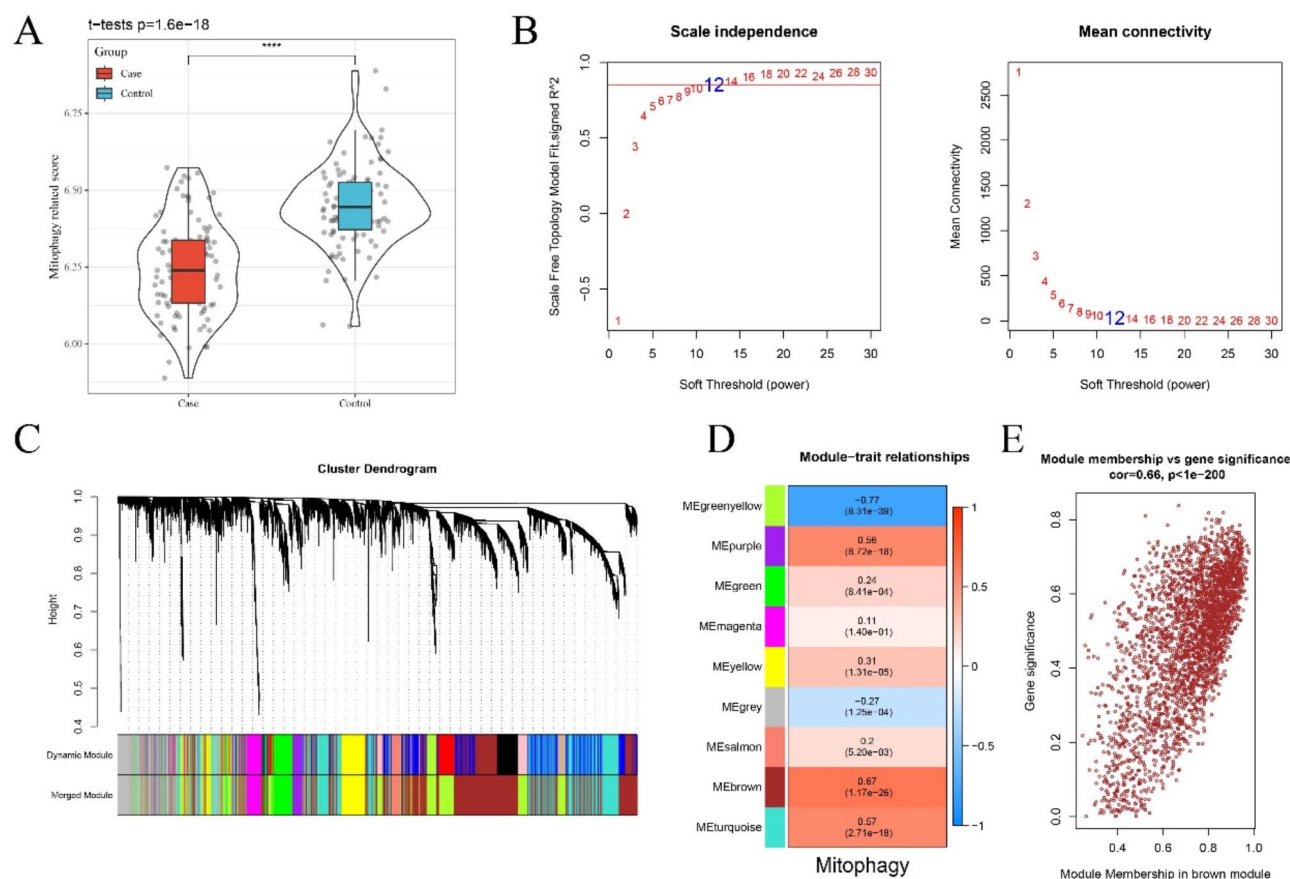


Fig. 1. Weighted co-expression network construction and key module identification in AD. (A) Box plot of ssGSEA results. (B) WGCNA soft threshold screening graph. (C) Dendrogram of all genes clustered based on a dissimilarity measure (1-TOM). (D) Module-trait correlation plot. (E) GS-MM plot of MEbrown modules.

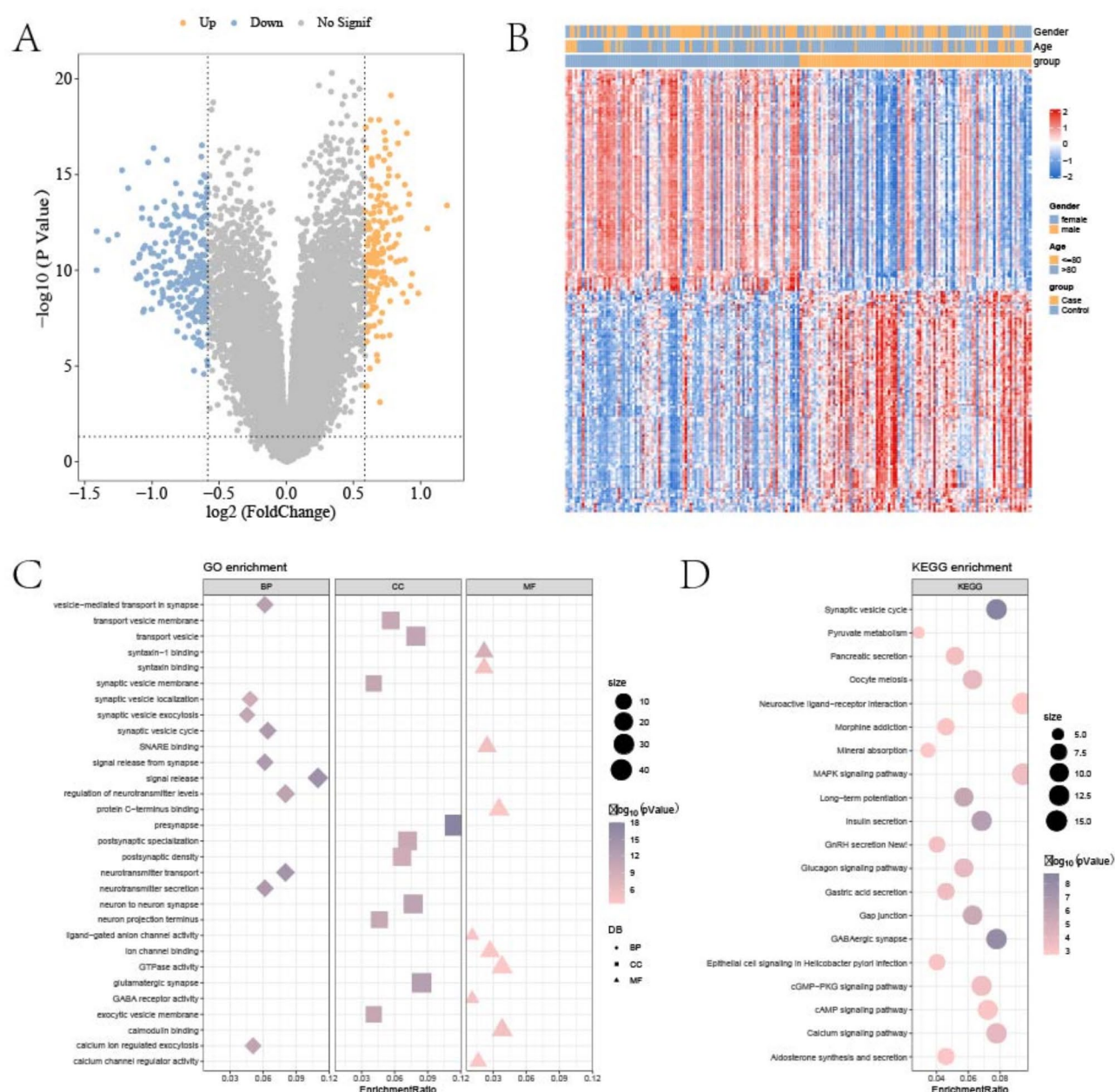


Fig. 2. Enrichment analysis of DEGs as well as GO and KEGG between AD and control samples. (A) Differential gene volcano plot. (B) Heatmap of the top 100 differential genes. (C) Differently expressed gene GO function analysis bubble chart. (D) Differently expressed gene KEGG functional analysis bubble plot.

insulin secretion, GABAergic synapses, long-term potentiation, and synaptic vesicle cycle (Fig. 2D). It was discovered that there was a notable enrichment of these genes to pathways associated with synaptic function.

Screening of MRGs-related signature genes

By taking the intersection of WGCNA-derived genes and DEGs, five overlapping genes were ultimately identified (Fig. 3A). LASSO regression and RFE techniques were employed to compress these 5 genes. Specifically, the model reached its optimal value in LASSO regression at $\lambda_{1se} = 0.1198712$ (Fig. 3B,C). Then, five candidate genes were selected based on their characteristics by RFE algorithm when the model error was minimized (Fig. 3D). Finally, by taking the intersection of the two machine learning experiments, the *YWHAZ* and *NDE1* genes were identified as biomarkers.

Diagnostic modeling and validation

A diagnostic prediction model for AD was created based on the *YWHAZ* and *NDE1* in the training set GSE132903. After plotting the ROC curves, the AUC values of *YWHAZ* and *NDE1* were calculated to be 0.777 and 0.793, respectively, which were both higher than 0.7 (Fig. 4A). This indicated that our signature genes can

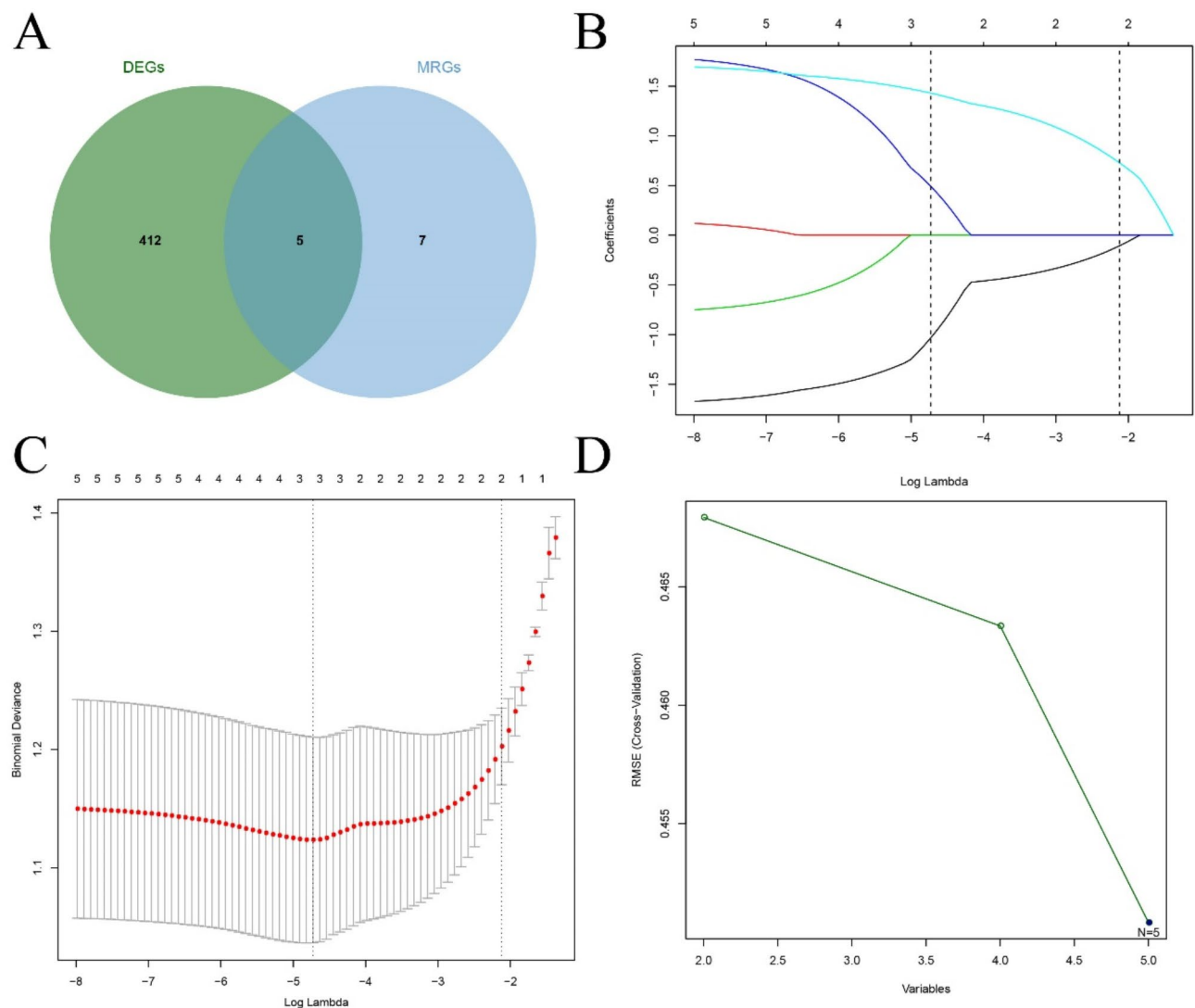


Fig. 3. Identification of characterized genes associated with MRGs in AD. **(A)** Venn diagram of the intersection of mitophagy-related modular genes and differential genes screened by WGCNA. **(B)** Trajectories of each independent variable with lambda. **(C)** Confidence intervals under lambda. **(D)** The plot of SVM-RFE pan error versus the number of features.

effectively diagnose AD. Subsequently, the results of ROC analysis showed that the area under the curve of the two-gene model was 0.796 (Fig. 4B), suggesting that a strong predictive ability of the model. Moreover, the mRNA expression of *YWHAZ* was significantly lower in AD samples than in control samples, while *NDE1* was high-expressed in AD samples (Fig. 4C). The prediction stability of the model gene in distinguishing AD from control samples was tested in the test set GSE122063 cohort with the same coefficients of the training set. It can be seen that the two genes had a strong predictive performance in the GSE122063 cohort, with an AUC value of 0.792 and 0.795 for *YWHAZ* and *NDE1*, respectively (Fig. 4D). The prediction was also accurate in the GSE122063 test (AUC = 0.848, Fig. 4E), further confirming the reliability of the diagnostic model. Similarly, the expression of *YWHAZ* was significantly lower in AD samples than in control samples, while the expression of *NDE1* was significantly higher in AD samples than in control samples (Fig. 4F). This suggested that *YWHAZ* and *NDE1* genes play different regulatory roles in the progression of AD.

TF-mRNA regulatory network analysis

The TFs of *YWHAZ* and *NDE1* genes were predicted using the NetworkAnalyst online tool, and a TF-mRNA interaction network was built using the JASPAR database. As shown in Fig. 5, the network consisted of 26 TFs and 2 hub genes. In particular, four TFs (*FOXC1*, *FOXL1*, *HOXA5*, and *GATA2*) were associated with both *YWHAZ* and *NDE1*, suggesting that they may play an important role in the two biomarkers targeting in AD.

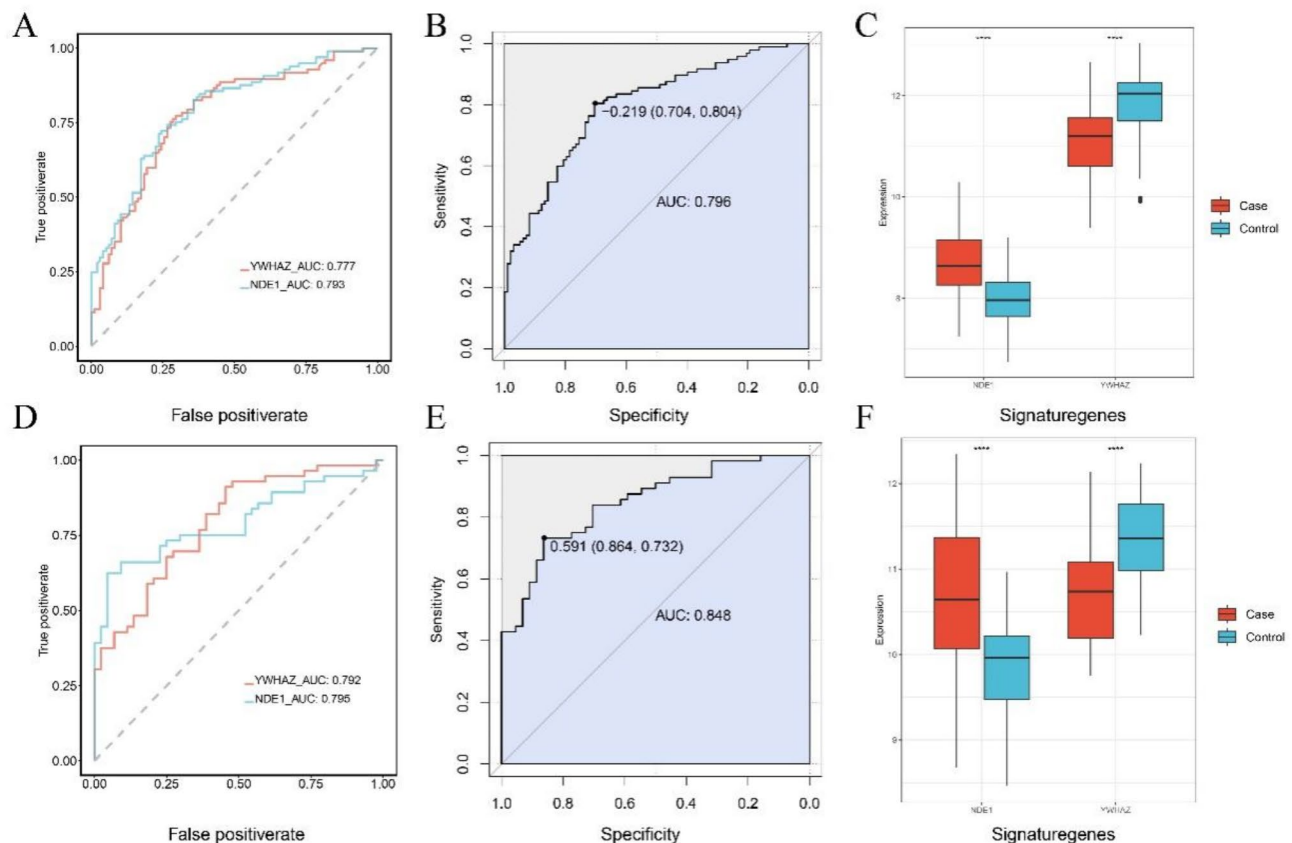


Fig. 4. Establishment as well as validation of diagnostic model based on MRGs-related signatures. (A) ROC curves for a single feature gene in the GSE132903 training set. (B) ROC curves of the combination of 2 feature genes in the GSE132903 training set. (C) Expression of hub genes in AD and control samples in the GSE132903 training set. (D) ROC curves for a single feature gene in the GSE122063 test set. (E) ROC curves for a combination of 2 feature genes in the GSE122063 test set. (F) Expression of hub genes in AD and control samples in the GSE122063 test set.

Immune cell infiltration and its correlation with biomarkers

The results of immune cell infiltration analysis showed that half of the immune cells, including natural killer cells, plasmacytoid dendritic cells, effector memory CD8 T cells, and Type 1 T helper cells, were considerably more abundant in control samples than in AD samples (Fig. 6A,B, $p < 0.05$). Next, the relationship between immunological scores and *YWHAZ* and *NDE1* was analyzed. The expression of *NDE1* was negatively correlated with the infiltration of activated CD4 T cells, effector memory CD4 T cells, memory B cells, regulatory T cells, and type 2 T helper cells (Fig. 6C, $p < 0.05$) but positively correlated with the infiltration of the rest immune cell types (Fig. 6C, $p < 0.05$). *YWHAZ* was positively related to the infiltration of activated CD4 T cells, effector memory CD4 T cells, memory B cells, type 2 T helper cells, and eosinophils but negatively related to the rest immune cell types (Fig. 6C, $p < 0.05$).

Correlation between the characteristic genes and pathways

The relationship between the *YWHAZ* and *NDE1* genes and the pathway scores was examined. It was found that *NDE1* was negatively correlated with the pathways MYC targets v1, spermatogenesis, pancreas beta-cells, and oxidative phosphorylation but positively correlated with the pathways mitotic spindle, wnt/beta-catenin signaling, p53 pathway and notch signaling (Fig. 7, $p < 0.05$). On the other hand, *YWHAZ* was positively correlated with wnt/beta-catenin signaling, p53 pathway, notch signaling and myogenesis but negatively correlated with the pathways MYC targets v1, oxidative phosphorylation, pancreas beta-cells and spermatogenesis (Fig. 7, $p < 0.05$). Based on the above results, it was speculated that *YWHAZ* and *NDE1* may have different effects on the occurrence and development of AD.

Discussion

AD is the primary cause of death for patients with dementia and at present there is no cure for it^{42,43}, necessitating the development of preventive and diagnostic methods for the disease. Though we currently still face a lack of molecular indicators for an accurate diagnosis of AD, research showed that AD pathogenesis is significantly influenced by neuronal mitophagy⁴⁴. Due to their high energy requirements, neurons are the most susceptible cell type to mitochondrial malfunction^{44,45}. Mitophagy may lead to neurological dysfunction because A β buildup in

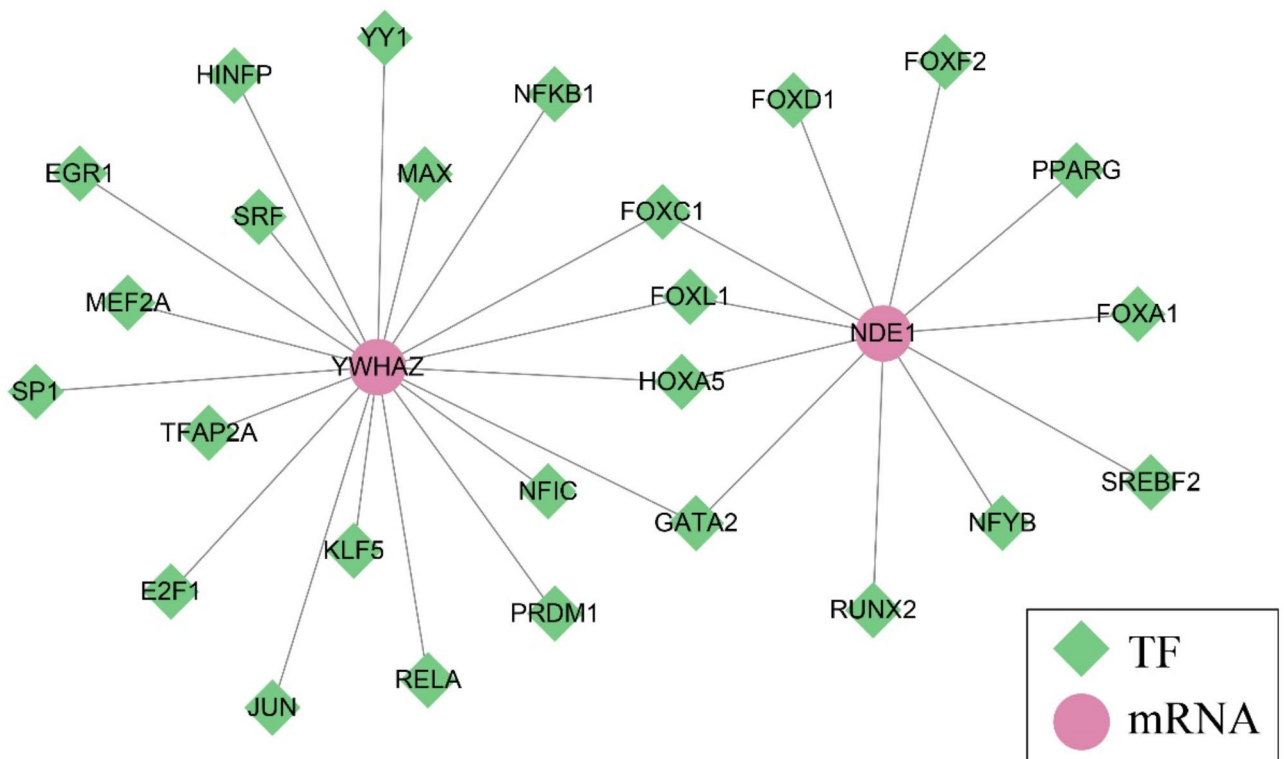


Fig. 5. Network diagram of TF and mRNA interactions. The purple dots in the figure represent mRNA molecules, while the green squares represent transcription factors.

the nervous system triggers cellular oxidative stress, a shortage of vital nutrients, and neuronal cell apoptosis⁴⁶. It has been proven that mitophagy lowers oxidative stress and eliminates damaged mitochondria, showing the potential to be developed as a preventive and therapeutic approach against neurodegenerative disorders. In the present work, *YWHAZ* and *NDE1*, which were identified as having potential for diagnosing AD, were identified as two MRGs by integrative analyses based on public databases.

Since the pathophysiology of AD is believed to be significantly influenced by mitophagy in neurons⁴⁴, building an AD prediction model with MRGs is a reliable method for clarifying the cause of AD and developing new treatment strategies. This study used machine learning experiments to identify *YWHAZ* and *NDE1* for an AD diagnostic model. A major protein implicated in numerous signal transduction pathways is 14-3-3 zeta protein isoform 1 (*YWHAZ*)⁴⁷. According to previous report, *YWHAZ* lowers the likelihood of AD by interacting with the tau gene in NFT, a distinctive neurohistological hallmark of AD⁴⁸. *YWHAZ* is directly associated with AD⁴⁹ because the protein expression of *YWHAZ* is downregulated in the hippocampus of AD patients and it may be a key regulatory gene in the prefrontal cortex of AD patients^{50,51}. This is consistent with the current finding that the expression of *YWHAZ* in AD samples was lower than that in control tissues. Neurodevelopmental protein 1 (*NDE1*) is, a protein-coding gene also known as nude, is thought to be a risk factor for major psychiatric illnesses and is substantially expressed in neurological and psychiatric diseases^{52,53}. Mutations in *NDE1* in mitochondria may stimulate the occurrence of multiple biosynthetic pathways that increase mitochondrial quality and quantity, including mitophagy⁵⁴. It was discovered that *NDE1* is crucial for microtubule organization, mitosis, and neural migration⁵⁵. Microtubule loss observed by Zempel et al. is a risk factor for the deterioration of AD⁵⁶. According to a study, a higher level of *NDE1* in AD might be caused by altered *NDE1* copy number in cortical neurons, which leads to poor neurodevelopment caused by secondary genomic mutations⁵⁷. *NDE1* has been shown to recruit LIS1 to dynein⁵⁸, and knockdown of *LIS1* can inhibit the retrograde movement of mitochondria in the axons of rat hippocampal neurons⁵⁹. Thus, screening crucial genes involved in mitophagy to prevent the development of AD is a promising strategy. The present work confirmed that *YWHAZ* and *NDE1* were closely associated with AD progression and had the potential to serve as biomarkers for AD.

The characterization of putative TF-mRNA regulation networks was also performed. Among the 26 TFs, *YWHAZ* and *NDE1* were linked to *FOXC1*, *FOXL1*, *HOXA5*, and *GATA2*. Forkhead box C1 (*FOXC1*), a TF of the forkhead box family, plays a regulatory role in cell viability and oxidative stress tolerance⁶⁰. Cerebellar structure develops relying on *FOXC1*, and the pathophysiology of Dandy-Walker deformity is linked to *FOXC1* deletion⁶¹. The forkhead box L1 (*FOXL1*) gene induces cell cycle arrest and death to suppressor cells, which facilitates brain development⁶². A major TF controlling neuronal shape is homology box A5 (*HOXA5*). In mice, disruption of *Hoxa5*-mediated neuronal morphogenesis can influence spatial learning and memory⁶³. Furthermore, tau neuropathology is closely involved in brain hypermethylation of the *HOXA* gene cluster⁶⁴. Contribution from hematology^{65,66} proposed GATA-binding protein 2 (*GATA2*) as a critical TF that controls

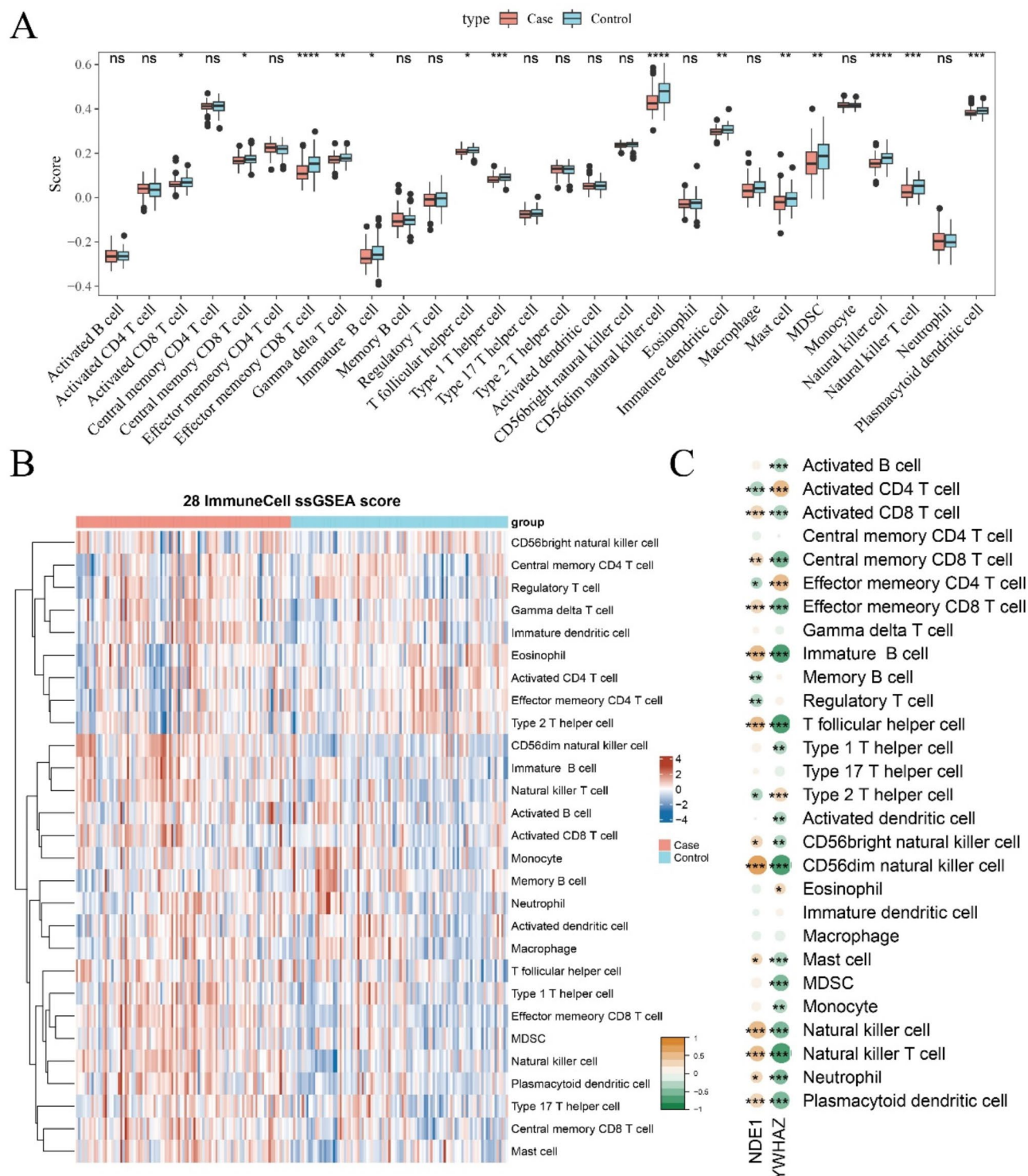


Fig. 6. Correlation of *YWHAZ* and *NDE1* genes with immune cell infiltration. (A, B) Differences in immune cell infiltration between AD and control. (C) Correlation of *YWHAZ* and *NDE1* genes with immune cells in AD (* represents whether it is significant or not, red–orange represents positive correlation and green represents negative correlation).

the expression of monoamine oxidase A in neurological and cardiovascular disorders⁶⁷. Hence, it is possible that these TFs fulfill unique regulatory functions in the initiation and progression of AD, albeit more research is required for confirmation.

Furthermore, GO and KEGG study revealed that the biological functions of DEGs were primarily enriched in pathways related to signaling and insulin secretion at synapses, long-term potentiation, and gap junction

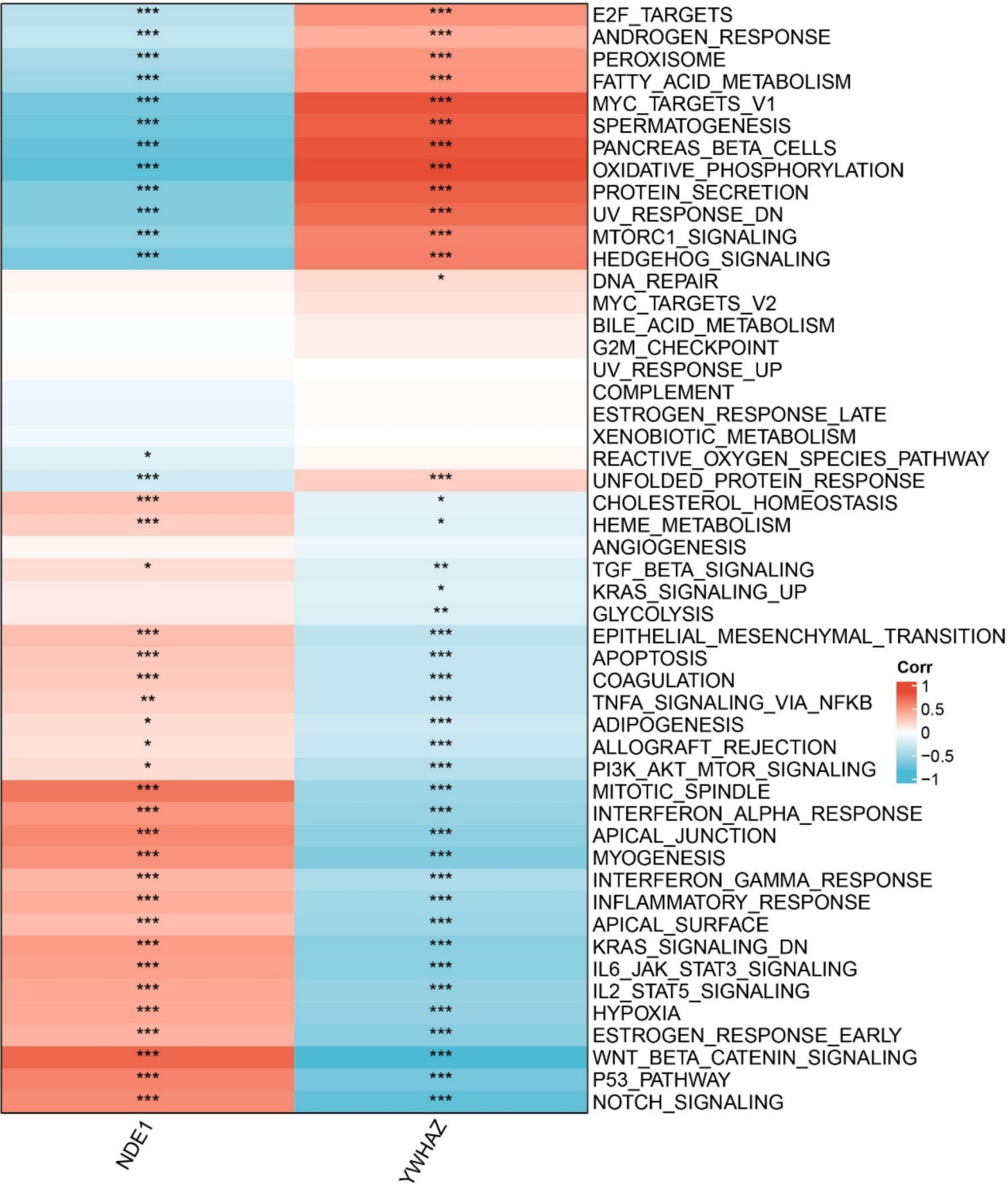


Fig. 7. Correlation between characteristic gene expression and pathways (* represents whether it is significant or not, red represents positive correlation and blue represents negative correlation).

pathways. These findings were consistent with some previous researches. For instance, synapses are found to be the basic building blocks of the brain, and synaptic activity promotes the development of new synapses and the maturation of mushroom-like spines^{68,69}. This process enhances the adaptation of synaptic strength to environmental changes and is crucial for learning and memory. Early AD patients' brains show a loss of synapses and disruption of synaptic activity⁷⁰. It has been confirmed that the primary cause of cognitive problems in AD patients is synapse loss and decreased synaptic activity⁷¹. According to past research, p-tau accumulation

causes mitochondrial abnormalities that trigger neuronal death⁹, while p-tau deficiency increases the body's release of insulin. Clinical research also demonstrated that blood glucose levels are lowered in AD patients, and that serum tau protein and blood glucose levels in healthy controls have a favorable correlation⁷². Furthermore, perturbations in neuronal Ca^{2+} levels caused by mitochondrial dysfunction in AD may lead to an imbalance in cell membrane, thereby causing neuronal death⁷³. Overall, these pathways may provide theoretical guidance and new insights for subsequent studies in AD.

This study examined the relationship between immune infiltration cells and diagnostic features. It was found that multiple immune cells, including activated CD8 T cell, central memory CD8 T cell, effector memory CD8 T cell, immature B cell, T follicular helper cell, and etc., were positively correlated with *NDE1* gene but negatively correlated with *YWHAZ*. However, the correlations were opposite for activated CD4 T cells and effector memory CD4 T cells. This indicated that these cells might play a part in the onset and progression of AD. Numerous studies indicated that CD4^+ T cells, CD8^+ T cells, and cytokines are involved in the pathogenesis of AD^{74,75}. CD4^+ T cells may orchestrate immunological systems, interact with microglia, and facilitate amyloid clearance, which could all lead to AD pathogenesis and offer therapeutic interventions⁷⁶. Clonally expanded CD8^+ T effector memory CD45RA^+ (TEMRA) cells were detected in the cerebrospinal fluid of patients with AD⁷⁷. CD8^+ TEMRA cells are negatively correlated with cognitive functions⁷⁸. In AD, disrupted balance between CD4^+ T cells and CD8^+ T cells may cause immune system dysregulation, which could promote or exacerbate the pathological process of AD⁷⁹. The expansion of B cells in AD promote the disease progression by producing immunoglobulins that are deposited around A β plaques, whereas therapeutic elimination of B cells can slow down AD deterioration^{80,81}. In summary, these studies suggested that *YWHAZ* and *NDE1* may influence the occurrence of AD by affecting immune infiltration.

According to the pathway enrichment scores, oxidative phosphorylation was negatively correlated with *NDE1* but positively correlated with *YWHAZ*, while opposite Wnt/ β -catenin signaling was positively correlated with *NDE1* but negatively correlated with *YWHAZ*. Activation of the wnt/ β -catenin pathway prevents the deposition of A β and p-tau, reduces neuroinflammation, and slows down the progression of AD^{82,83}. Wnt signaling can maintain and even restore the blood–brain barrier (BBB) properties of endothelial cells (ECs), thus influencing the occurrence of AD⁸⁴. Some studies have also found that restoring Wnt/ β -catenin signaling is a promising therapeutic strategy for AD⁸⁵. Abnormal oxidative phosphorylation will cause A β deposition and tau hyperphosphorylation, facilitating the onset of AD⁸⁶. As previously mentioned, *NDE1* is closely associated with mitochondrial mutations. Previous research revealed that genes involved in OxPhos, including those participating in complexes II and V, are significantly downregulated in AD subjects⁸⁷. In fact, mitochondrial dysfunction may lead to energy failure in neurons, thereby inducing synaptic dysfunction in cognitive impairment⁸⁸. These results suggested that *YWHAZ* and *NDE1* may influence the development of AD through these pathways.

It is also equally important to acknowledge the limitations of our study. Firstly, only a small number of patients from public databases were analyzed as the basis to support our findings. To address this, future studies could expand our sample size by including a more diverse cohort of patients from multiple sources (both domestic and international). Secondly, prospective investigations are required to rule out potential bias caused by retrospective recruitment of patients. In addition, the role of the two MRGs identified by this study for AD mitophagy should be verified by in vivo animal experiment in animals and in vitro cell experiments. Finally, further research is required to examine the relationship between AD hallmark genes and immune cell infiltration.

Conclusion

This study developed a diagnostic model based on two hallmark genes linked to mitophagy in AD using machine learning algorithms. The level of immunological infiltration and biochemical pathways in AD patients were accurately predicted by the two signature genes, which showed a strong predictive potential in both AD and control samples. In summary, investigation into the characteristics of mitophagy may provide theoretical guidance for exploring the mechanisms of AD occurrence and development.

Data availability

The datasets generated and/or analyzed during the current study are available in the [GSE122063] repository, [<https://www.ncbi.nlm.nih.gov/geo/query/acc.cgi?acc=GSE122063>] and [GSE132903] repository, [<https://www.ncbi.nlm.nih.gov/geo/query/acc.cgi?acc=GSE132903>].

Received: 11 November 2024; Accepted: 10 February 2025

Published online: 27 March 2025

References

1. Monica Moore, M., Díaz-Santos, M. & Vossel, K. *Alzheimer's Association 2021 Facts and Figures Report* (Alzheimer's Association, 2021).
2. 2021 Alzheimer's disease facts and figures. *Alzheimers Dement.*;17(3):327–406 (2021).
3. Arvanitakis, Z., Shah, R. C. & Bennett, D. A. Diagnosis and management of dementia: Review. *JAMA*. **322**(16), 1589–1599 (2019).
4. Brookmeyer, R., Johnson, E., Ziegler-Graham, K. & Arrighi, H. M. Forecasting the global burden of Alzheimer's disease. *Alzheimers Dement.* **3**(3), 186–191 (2007).
5. Bateman, R. J., Barthelemy, N. R. & Horie, K. Another step forward in blood-based diagnostics for Alzheimer's disease. *Nat. Med.* **26**(3), 314–316 (2020).
6. Bateman, R. J. et al. Clinical and biomarker changes in dominantly inherited Alzheimer's disease. *N. Engl. J. Med.* **367**(9), 795–804 (2012).
7. Zarini-Gakiye, E., Amini, J., Sanadgol, N., Vaezi, G. & Parivar, K. Recent updates in the Alzheimer's disease etiopathology and possible treatment approaches: A narrative review of current clinical trials. *Curr. Mol. Pharmacol.* **13**(4), 273–294 (2020).

8. Mattson, M. P., Gleichmann, M. & Cheng, A. Mitochondria in neuroplasticity and neurological disorders. *Neuron*. **60**(5), 748–766 (2008).
9. Kerr, J. S. et al. Mitophagy and Alzheimer's disease: Cellular and molecular mechanisms. *Trends Neurosci.* **40**(3), 151–166 (2017).
10. Xu, X. et al. Bushen Yizhi Formula regulates the IRE1 α pathway to alleviate endoplasmic reticulum stress in an Alzheimer's disease rat model. *Biocell* **47**(7), 1595–1609 (2023).
11. Menzies, F. M., Fleming, A. & Rubinsztein, D. C. Compromised autophagy and neurodegenerative diseases. *Nat. Rev. Neurosci.* **16**(6), 345–357 (2015).
12. Cai, Q. & Tammineni, P. Alterations in mitochondrial quality control in Alzheimer's disease. *Front. Cell Neurosci.* **10**, 24 (2016).
13. Rubinsztein, D. C., Marino, G. & Kroemer, G. Autophagy and aging. *Cell* **146**(5), 682–695 (2011).
14. Palikaras, K., Lionaki, E. & Tavernarakis, N. Coordination of mitophagy and mitochondrial biogenesis during ageing in *C. elegans*. *Nature* **521**(7553), 525–528 (2015).
15. Fang, E. F. et al. Mitophagy inhibits amyloid-beta and tau pathology and reverses cognitive deficits in models of Alzheimer's disease. *Nat. Neurosci.* **22**(3), 401–412 (2019).
16. Foote, H. P. et al. Using pharmacokinetic modeling and electronic health record data to predict clinical and safety outcomes after methylprednisolone exposure during cardiopulmonary bypass in neonates. *Congenit. Heart Dis.* **18**(3), 295–313 (2023).
17. Piras, I. S. et al. Transcriptome changes in the Alzheimer's disease middle temporal gyrus: Importance of RNA metabolism and mitochondria-associated membrane genes. *J. Alzheimers Dis.* **70**(3), 691–713 (2019).
18. McKay, E. C. et al. Peri-infarct upregulation of the oxytocin receptor in vascular dementia. *J. Neuropathol. Exp. Neurol.* **78**(5), 436–452 (2019).
19. Xu, W. et al. The prognostic value and clinical significance of mitophagy-related genes in hepatocellular carcinoma. *Front. Genet.* **13**, 917584 (2022).
20. Langfelder, P. & Horvath, S. WGCNA: An R package for weighted correlation network analysis. *BMC Bioinform.* **9**, 559 (2008).
21. Li, D. et al. Human skin long noncoding RNA WAKMAR1 regulates wound healing by enhancing keratinocyte migration. *Proc. Natl. Acad. Sci. U. S. A.* **116**(19), 9443–9452 (2019).
22. Zhang, J. et al. Screening of potential biomarkers in the peripheral serum for steroid-induced osteonecrosis of the femoral head based on WGCNA and machine learning algorithms. *Dis. Mark.* **2022**, 2639470 (2022).
23. Saunders, M. A., Liang, H. & Li, W. H. Human polymorphism at microRNAs and microRNA target sites. *Proc. Natl. Acad. Sci. U. S. A.* **104**(9), 3300–3305 (2007).
24. Szklarczyk, D. et al. The STRING database in 2023: Protein-protein association networks and functional enrichment analyses for any sequenced genome of interest. *Nucleic Acids Res.* **51**(D1), D638–D646 (2023).
25. Gautier, L., Cope, L., Bolstad, B. M. & Irizarry, R. A. affy-analysis of Affymetrix GeneChip data at the probe level. *Bioinformatics* **20**(3), 307–315 (2004).
26. Ali, A., Ajil, A., Meenakshi Sundaram, A. & Joseph, N. Detection of gene ontology clusters using biclustering algorithms. *SN Comput. Sci.* <https://doi.org/10.1007/s42979-022-01624-w> (2023).
27. Ali, A., Hulipalled, V. R., Patil, S. S. & Abdulkader, R. DPEBic: detecting essential proteins in gene expressions using encoding and biclustering algorithm. *J. Ambient. Intell. Humaniz. Comput.* <https://doi.org/10.1007/s12652-021-03036-9> (2021).
28. Ramachandra, H. V., Ali, A., Ambili, P. S., Thota, S., Asha, P. N., (eds). An optimization on bicluster algorithm for gene expression data. In *2023 4th IEEE Global Conference for Advancement in Technology (GCAT)*, (2023).
29. Ritchie, M. E. et al. limma powers differential expression analyses for RNA-sequencing and microarray studies. *Nucleic Acids Res.* **43**(7), e47 (2015).
30. Gustavsson, E. K., Zhang, D., Reynolds, R. H., Garcia-Ruiz, S. & Ryten, M. ggtranscript: An R package for the visualization and interpretation of transcript isoforms using ggplot2. *Bioinformatics* **38**(15), 3844–3846 (2022).
31. Friedman, J., Hastie, T. & Tibshirani, R. Regularization paths for generalized linear models via coordinate descent. *J. Stat. Softw.* **33**(1), 1–22 (2010).
32. Blanche, P., Dartigues, J. F. & Jacqmin-Gadda, H. Estimating and comparing time-dependent areas under receiver operating characteristic curves for censored event times with competing risks. *Stat. Med.* **32**(30), 5381–5397 (2013).
33. Shannon, P. et al. Cytoscape: A software environment for integrated models of biomolecular interaction networks. *Genome Res.* **13**(11), 2498–2504 (2003).
34. Barbie, D. A. et al. Systematic RNA interference reveals that oncogenic KRAS-driven cancers require TBK1. *Nature* **462**(7269), 108–112 (2009).
35. Charoentong, P. et al. Pan-cancer immunogenomic analyses reveal genotype-immunophenotype relationships and predictors of response to checkpoint blockade. *Cell Rep.* **18**(1), 248–262 (2017).
36. Kanehisa, M. & Goto, S. KEGG: Kyoto encyclopedia of genes and genomes. *Nucleic Acids Res.* **28**(1), 27–30 (2000).
37. Kanehisa, M., Sato, Y., Kawashima, M., Furumichi, M. & Tanabe, M. KEGG as a reference resource for gene and protein annotation. *Nucleic Acids Res.* **44**(D1), D457–D462 (2016).
38. Kanehisa, M. Toward understanding the origin and evolution of cellular organisms. *Protein Sci.* **28**(11), 1947–1951 (2019).
39. Kanehisa, M., Furumichi, M., Sato, Y., Kawashima, M. & Ishiguro-Watanabe, M. KEGG for taxonomy-based analysis of pathways and genomes. *Nucleic Acids Res.* **51**(D1), D587–D592 (2022).
40. Yu, G., Wang, L. G., Han, Y. & He, Q. Y. clusterProfiler: An R package for comparing biological themes among gene clusters. *Omics* **16**(5), 284–287 (2012).
41. Hänzelmann, S., Castelo, R. & Guinney, J. GSVA: Gene set variation analysis for microarray and RNA-seq data. *BMC Bioinform.* **14**, 7 (2013).
42. Kumar, M. & Bansal, N. A revisit to etiopathogenesis and therapeutic strategies in Alzheimer's disease. *Curr. Drug Targets.* **23**(5), 486–512 (2022).
43. Gao, Y., Wen, D., Wang, S. & Wang, J. Presenilin and Alzheimer's disease interactions with aging, exercise and high-fat diet: A systematic review. *Biocell* **47**(1), 41–49 (2023).
44. Shefa, U. et al. Mitophagy links oxidative stress conditions and neurodegenerative diseases. *Neural Regen. Res.* **14**(5), 749–756 (2019).
45. Jayadev, S. & Yusuff, I. Robust U-HPLC method development of desonide and its application to in vitro release testing (IVRT) of topical cream products. *Curr. Pharm. Anal.* **20**(5), 327–344 (2024).
46. Reddy, P. H. & Oliver, D. M. Amyloid beta and phosphorylated tau-induced defective autophagy and mitophagy in Alzheimer's disease. *Cells* **8**(5), 488 (2019).
47. Aitken, A. 14-3-3 proteins: A historic overview. *Semin. Cancer Biol.* **16**(3), 162–172 (2006).
48. Miller, J. A., Oldham, M. C. & Geschwind, D. H. A systems level analysis of transcriptional changes in Alzheimer's disease and normal aging. *J. Neurosci.* **28**(6), 1410–1420 (2008).
49. Ni, P., Pan, K. & Zhao, B. Influence of N6-methyladenosine (m6A) modification on cell phenotype in Alzheimer's disease. *PLOS ONE* **18**(8), e0289068 (2023).
50. Yang, F. et al. Identification of key regulatory genes and pathways in prefrontal cortex of Alzheimer's disease. *Interdiscip. Sci.* **12**(1), 90–98 (2020).
51. Ho Kim, J. et al. Proteome-wide characterization of signalling interactions in the hippocampal CA4/DG subfield of patients with Alzheimer's disease. *Sci. Rep.* **5**(1), 11138 (2015).

52. Bradshaw, N. J. & Hayashi, M. A. NDE1 and NDEL1 from genes to (mal)functions: parallel but distinct roles impacting on neurodevelopmental disorders and psychiatric illness. *Cell Mol. Life Sci.* **74**(7), 1191–1210 (2017).
53. Ogawa, F. et al. NDE1 and GSK3 β associate with TRAK1 and regulate axonal mitochondrial motility: Identification of cyclic AMP as a novel modulator of axonal mitochondrial trafficking. *ACS Chem Neurosci.* **7**(5), 553–564 (2016).
54. Amine, A. A. A., Liao, C. W., Hsu, P. C., Opoc, F. J. G. & Leu, J. Y. Experimental evolution improves mitochondrial genome quality control in *Saccharomyces cerevisiae* and extends its replicative lifespan. *Curr. Biol.* **31**(16), 3663–3670 (2021).
55. Murphy, L. C. & Millar, J. K. Regulation of mitochondrial dynamics by DISC1, a putative risk factor for major mental illness. *Schizophr. Res.* **187**, 55–61 (2017).
56. Zempel, H. & Mandelkow, E. M. Linking amyloid- β and tau: Amyloid- β induced synaptic dysfunction via local wreckage of the neuronal cytoskeleton. *Neurodegener. Dis.* **10**(1–4), 64–72 (2012).
57. Allach El Khattabi, L. et al. 16p13.11 microduplication in 45 new patients: refined clinical significance and genotype-phenotype correlations. *J. Med. Genet.* **57**(5), 301–307 (2020).
58. McKenney, R. J., Vershinin, M., Kunwar, A., Vallee, R. B. & Gross, S. P. LIS1 and NudE induce a persistent dynein force-producing state. *Cell* **141**(2), 304–314 (2010).
59. Shao, C.-Y. et al. Distinct functions of nuclear distribution proteins LIS1, Ndel1 and NudCL in regulating axonal mitochondrial transport. *Traffic* **14**(7), 785–797 (2013).
60. Berry, F. B. et al. FOXO1 is required for cell viability and resistance to oxidative stress in the eye through the transcriptional regulation of FOXO1A. *Hum. Mol. Genet.* **17**(4), 490–505 (2008).
61. Haldipur, P. et al. Phenotypic outcomes in Mouse and Human Foxc1 dependent Dandy–Walker cerebellar malformation suggest shared mechanisms. *Elife* <https://doi.org/10.7554/eLife.20898> (2017).
62. Chen, X. et al. Inhibitory effects of forkhead box L1 gene on osteosarcoma growth through the induction of cell cycle arrest and apoptosis. *Oncol. Rep.* **34**(1), 265–271 (2015).
63. Hou, Y., Yan, W., Guo, L., Li, G. & Sang, N. Prenatal PM(2.5) exposure impairs spatial learning and memory in male mice offspring: From transcriptional regulation to neuronal morphogenesis. *Part. Fibre Toxicol.* **20**(1), 13 (2023).
64. Lunnon, K. et al. Methylomic profiling implicates cortical deregulation of ANK1 in Alzheimer's disease. *Nat. Neurosci.* **17**(9), 1164–1170 (2014).
65. Katerndahl, C. D. S. et al. Tumor suppressor function of Gata2 in acute promyelocytic leukemia. *Blood* **138**(13), 1148–1161 (2021).
66. Qiu, C. et al. The critical role of SENP1-mediated GATA2 deSUMOylation in promoting endothelial activation in graft arteriosclerosis. *Nat. Commun.* **8**, 15426 (2017).
67. Gupta, V., Khan, A. A., Sasi, B. K. & Mahapatra, N. R. Molecular mechanism of monoamine oxidase A gene regulation under inflammation and ischemia-like conditions: Key roles of the transcription factors GATA2, Sp1 and TBP. *J. Neurochem.* **134**(1), 21–38 (2015).
68. Saneyoshi, T. et al. Activity-dependent synaptogenesis: Regulation by a CaM-kinase kinase/CaM-kinase I/ β PIX signaling complex. *Neuron* **57**(1), 94–107 (2008).
69. Ryan, T. J., Roy, D. S., Pignatelli, M., Arons, A. & Tonegawa, S. Engram cells retain memory under retrograde amnesia. *Science* **348**(6238), 1007–1013 (2015).
70. Selkoe, D. J. Alzheimer's disease is a synaptic failure. *Science* **298**(5594), 789–791 (2002).
71. Terry, R. D. et al. Physical basis of cognitive alterations in Alzheimer's disease: Synapse loss is the major correlate of cognitive impairment. *Ann. Neurol.* **30**(4), 572–580 (1991).
72. Mangiafico, S. P. et al. Tau suppresses microtubule-regulated pancreatic insulin secretion. *Mol. Psychiatry* **28**(9), 3982–3993 (2023).
73. Bezprozvanny, I. & Mattson, M. P. Neuronal calcium mishandling and the pathogenesis of Alzheimer's disease. *Trends Neurosci.* **31**(9), 454–463 (2008).
74. Lueg, G. et al. Clinical relevance of specific T-cell activation in the blood and cerebrospinal fluid of patients with mild Alzheimer's disease. *Neurobiol. Aging* **36**(1), 81–89 (2015).
75. Ye, X. et al. Interleukin-17 promotes the infiltration of CD8 $^{+}$ T cells into the brain in a mouse model for Alzheimer's Disease. *Immunol. Invest.* **52**(2), 135–153 (2023).
76. Mittal, K. et al. CD4 $^{+}$ T cells induce a subset of MHCII-expressing microglia that attenuates Alzheimer pathology. *iScience* **16**, 298–311 (2019).
77. Gate, D. et al. Clonally expanded CD8 T cells patrol the cerebrospinal fluid in Alzheimer's disease. *Nature* **577**(7790), 399–404 (2020).
78. McManus, R. M. & Heneka, M. T. T cells in Alzheimer's disease: Space invaders. *Lancet Neurol.* **19**(4), 285–287 (2020).
79. Afsar, A., Chen, M., Xuan, Z. & Zhang, L. A glance through the effects of CD4 $^{+}$ T cells, CD8 $^{+}$ T cells, and cytokines on Alzheimer's disease. *Comput. Struct. Biotechnol. J.* **21**, 5662–5675 (2023).
80. Kim, K. et al. Therapeutic B-cell depletion reverses progression of Alzheimer's disease. *Nat. Commun.* **12**(1), 2185 (2021).
81. Sollvander, S. et al. Increased number of plasma B cells producing autoantibodies against A β 42 protofibrils in Alzheimer's disease. *J. Alzheimers Dis.* **48**(1), 63–72 (2015).
82. Yoon, M. et al. Inhibition of CXXC5 function rescues Alzheimer's disease phenotypes by restoring Wnt/ β -catenin signaling pathway. *Pharmacol. Res.* **194**, 106836 (2023).
83. Liu, J. et al. Icarin ameliorates glycolytic dysfunction in Alzheimer's disease models by activating the Wnt/ β -catenin signaling pathway. *FEBS J.* **291**(10), 2221–2241 (2024).
84. Liu, L., Wan, W., Xia, S., Kalionis, B. & Li, Y. Dysfunctional Wnt/ β -catenin signaling contributes to blood–brain barrier breakdown in Alzheimer's disease. *Neurochem. Int.* **75**, 19–25 (2014).
85. Jia, L., Piña-Crespo, J. & Li, Y. Restoring Wnt/ β -catenin signaling is a promising therapeutic strategy for Alzheimer's disease. *Mol. Brain.* **12**(1), 104 (2019).
86. Roy, R. G., Mandal, P. K. & Maroon, J. C. Oxidative stress occurs prior to amyloid β plaque formation and tau phosphorylation in Alzheimer's disease: Role of glutathione and metal ions. *ACS Chem. Neurosci.* **14**(17), 2944–2954 (2023).
87. Mastroeni, D. et al. Nuclear but not mitochondrial-encoded oxidative phosphorylation genes are altered in aging, mild cognitive impairment, and Alzheimer's disease. *Alzheimers Dement.* **13**(5), 510–519 (2017).
88. Elmore, S. E. & La Merrill, M. A. Oxidative phosphorylation impairment by DDT and DDE. *Front. Endocrinol.* <https://doi.org/10.3389/fendo.2019.00122> (2019).

Acknowledgements

None

Author contributions

All authors contributed to this present work: [JRL], [MY] and [YL] designed the research; [LHC] and [WHY] performed interpreted the results; [WHY] and [YL] performed the experiments and analyzed the results; [JRL], [MY], [YL] and [WHY] drafted the manuscript; [JRL], [MY] and [LHC] revised the manuscript and gave the final approval of the version to be published. All authors read and approved the final manuscript.

Funding

The authors declare that they have received no funding.

Declarations

Competing interests

The authors declare no competing interests.

Additional information

Supplementary Information The online version contains supplementary material available at <https://doi.org/10.1038/s41598-025-89980-4>.

Correspondence and requests for materials should be addressed to J.L., W.Y. or Y.L.

Reprints and permissions information is available at www.nature.com/reprints.

Publisher's note Springer Nature remains neutral with regard to jurisdictional claims in published maps and institutional affiliations.

Open Access This article is licensed under a Creative Commons Attribution-NonCommercial-NoDerivatives 4.0 International License, which permits any non-commercial use, sharing, distribution and reproduction in any medium or format, as long as you give appropriate credit to the original author(s) and the source, provide a link to the Creative Commons licence, and indicate if you modified the licensed material. You do not have permission under this licence to share adapted material derived from this article or parts of it. The images or other third party material in this article are included in the article's Creative Commons licence, unless indicated otherwise in a credit line to the material. If material is not included in the article's Creative Commons licence and your intended use is not permitted by statutory regulation or exceeds the permitted use, you will need to obtain permission directly from the copyright holder. To view a copy of this licence, visit <http://creativecommons.org/licenses/by-nc-nd/4.0/>.

© The Author(s) 2025